ELSEVIER

Journal of Hydrology 266 (2002) 40–52

Journal of Hydrology

www.elsevier.com/locate/jhydrol

Stochastic optimization for global minimization and geostatistical calibration

Minchul Jang*, Jonggeun Choe

School of Civil, Urban and Geosystems Engineering, Seoul National University, San 56-1 Shinlim-Dong, Kwanak-Gu, Seoul 151-742, South Korea

Received 5 September 2001; revised 7 May 2002; accepted 14 May 2002

Abstract

This study proposes a stochastic optimization technique that uses a gradient-based method as the primary optimization method, as well as a geostatistical conditional simulation to perturb and calibrate parameters at every local minimum. If the optimization process is trapped at a local minimum due to the limitations of the gradient-based method, it generates equi-probable parameter fields using a geostatistical conditional simulation. Among the generated fields, the optimization process selects one that enables the objective function to be reduced below the value of that at the local minimum, and then reactivates the gradient-based optimization. In generating equi-probable parameter fields, a constrained number of points (noted as releasing points) are randomly selected, and spatially correlated values are generated at the releasing points, conditioned to optimum parameters at the local minimum.

By applying the stochastic optimization to synthetic permeability fields, it is observed that an inversed permeability field reproduces not only global distribution but also local spatial variability of the reference fields. In addition, the pressure distributions of the inversed and the reference field were much alike. To investigate dynamic properties of the inversed field and the reference field, streamline simulation was performed on both fields. Streamlines of the inversed field showed similar trajectories to those of the reference field, and time of flight (TOF) distribution of the inversed field was analogous to that of the reference field.

The stochastic optimization technique proposed in this paper enables an inverse process to converge to a global minimum while preserving geostatistical properties such as mean, standard deviation, and variogram of an original field. Therefore, the stochastic optimization will be efficient in predicting future performance of a field from constrained number of permeability and pressure observation data.

Keywords: Streamline simulation; Stochastic optimization; Global minimization

1. Introduction

To predict reliable future performances of a reservoir or an aquifer, it is indispensable to generate an accurate simulation model honoring all available data such as core data, pressure data, seismic data, and so on. Integration of additional data reduces the uncertainty while enhancing the accuracy of the model (Wen et al., 1998). Among various reservoir parameters, permeability is one of the most important that governs reservoir or aquifer performance (McLaughlin and Townly, 1996).

* Corresponding author. Fax: +82-2-871-8938.
E-mail addresses: jmc@geofluid.snu.ac.kr (M. Jang), johnchoe@snu.ac.kr (J. Choe).

0022-1694/02/$ - see front matter
PII: S0022-1694(02)00115-4

Geostatistical techniques provide efficient ways for identifying parameters of an unknown field. By using conditional simulations such as sequential Gaussian simulation (SGS) and sequential indicator simulation (SIS), multiple equi-probable distributions of unknown parameters from constrained sample data can be obtained (Deutsch, 1997). They can be good estimates of the field, but it is often required to select an optimal one reflecting not only spatial but also dynamic information of the field.

Optimization techniques make it possible for a model to honor the given static and dynamic information. Optimization techniques can be largely categorized into gradient-based and non-gradient methods. Although gradient-based methods are mathematically straightforward and computationally efficient compared to the non-gradient methods, the local minimum problem has been one of the fatal drawbacks of the gradient-based methods (Sun, 1994). Therefore, we propose a new optimization technique aided by geostatistical methods to overcome the local minimum problem in gradient-based optimization techniques.

Several works have been attempted to couple geostatistical methods with inverse techniques. RamaRao et al. (1995) proposed the pilot point method that generates an ensemble of permeability fields conditioned to both permeability and pressure measurements. In their work, they generated a selected number of conditionally simulated transmissivity fields and calibrated each of the fields to match the pressure observations. The calibration phase involves adding pilot points to the transmissivity dataset for producing a revised conditional simulation.

Gomez-Hernandez et al. (1997) proposed the sequential self-calibration (SSC) method. A transmissivity field is generated conditional to the given permeability data, and the field is then modified until the pressure data are also honored. They employed the concept of master locations at which perturbations of transmissivity are determined to enhance the misfit between observed and calculated pressures. Then, the perturbations are propagated to the rest of the domain by Kriging (Wen et al., 1996; Wen et al., 1998).

Zimmerman et al. (1998) presented the comparison of geostatistically based inverse methods including the pilot points method and the SSC method for modeling groundwater flow. The comparisons of the method outcomes were based on the prediction of travel times and travel paths taken by conservative solutes migrating in an aquifer. The research showed the effectiveness and applicability of geostatistical approaches for inverse problems.

Geostatistically based methods such as SSC and the pilot points method, consist of two main stages. These are generation of multiple fields conditioned to the given transmissivity data and the subsequent calibration of the fields to honor head observations. To condition the fields to head observations, gradient-based optimization was used in both the SSC and the pilot point method. This results in incomplete conditioning due to the limitation of the gradient-based optimization method, specifically the local minimum problem. In addition, those methods are highly sensitive to initial fields, and the optimized fields are necessarily dependent on the initial fields generated by multiple realization. This paper proposes an optimization technique which can overcome the local minimum problem, and which is less sensitive to an initial field by starting from Kriging in the replacement of multiple realizations for the initial field.

In the meantime, all inverse processes perform quite a number of forward simulations and accompany sensitivity computation internally and iteratively, so inverse modeling needs enormous computational effort. Due to these facts, many studies have focused on how to enhance efficiency in forward simulation and sensitivity computation (Vasco et al., 1999; Wu et al., 1999).

In recent decades, streamline simulation has been widely used to predict oil recovery in reservoir simulations. The quickness and effectiveness of streamline simulation make it possible to simulate reservoirs of multi-million cells and to develop fine-scale models that integrate detailed three-dimensional geologic and geophysical data (Datta-Gupta et al., 1998; King and Datta-Gupta, 1998). Another advantage of the streamline simulation is that the stability constraint of the underlying gird can be effectively relieved by solving one-dimensional equations along streamlines (Batycky et al., 1997; Thiele et al., 1996). Batycky et al. (1997) developed a three-dimensional and multi-phase reservoir simulator. The model eliminated the numerical dispersion error and was

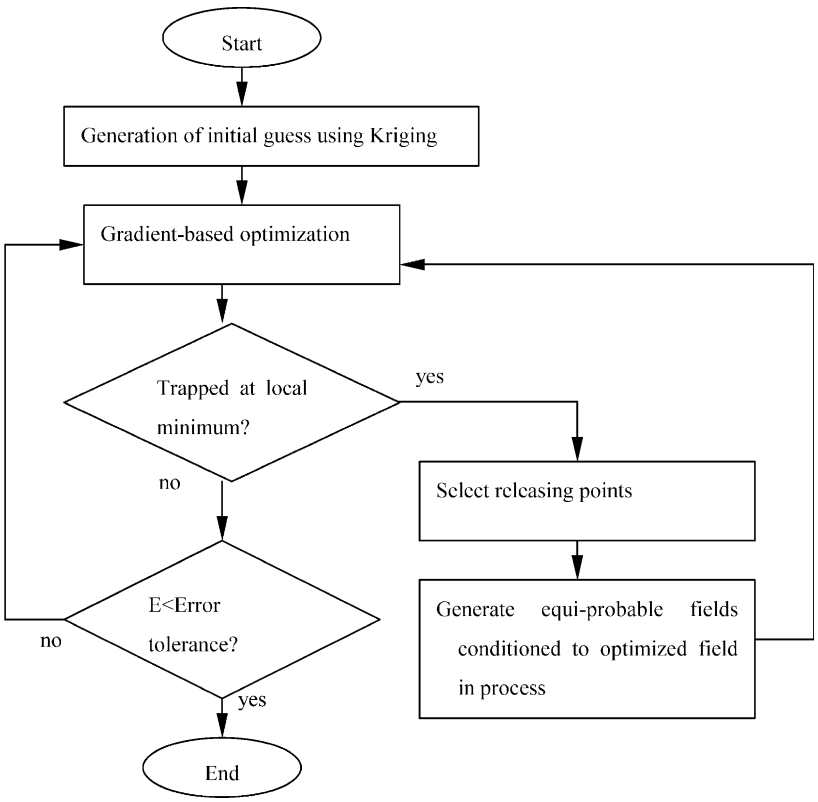

Fig. 1. Overview of the stochastic optimization algorithm.

10–1000 times faster than existing conventional reservoir simulators.

Sensitivity coefficients play an important role in solving an inverse problem. At every iteration step in a gradient-based optimization process, it is necessary to compute the gradient of an objective function or sensitivity coefficients newly. As a result, it makes the whole inverse process time consuming. In the adjoint state method, the flow problem and the adjoint sensitivity problem have the same form, so the calculation of the sensitivity coefficients is straightforward and very efficient (Sykes, 1985). If the number of parameters to be identified is greater than the number of the observation data, which is usually the case, the adjoint state method is known to be more advantageous than other methods such as the influence coefficient method and the sensitivity equation method (Dogru and Seinfeld, 1981). The adjoint state method allows a stable and quick solution to the time consuming inverse problems.

To observe the applicability of the proposed method, a synthetic permeability field was generated and used as the reference field to be identified. Most previous studies validated their inverse models mainly by showing the overall similarity between a synthetic permeability field and an inversed permeability field. For model performance, they presented an analogy of production history, tracer breakthrough curve, and producing water cut, etc. Although these properties represent the overall characteristics of aquifer or reservoir performance, they are not sufficient to describe spatial characteristics of model performance. We investigated model performances from the spatial point of view, such as pressure distribution, streamline trajectories, and time of flight (TOF) distributions of a synthetic and an inversed field.

To enhance computational efficiency, streamline simulation was implemented for fast and efficient forward simulation. To achieve fast computation of sensitivity, an adjoint state equation was derived for

the applied system, which have constant pressure boundary conditions at injection and production wells.

2. Stochastic optimization

Gradient-based optimization techniques are mathematically reasonable and fast in computation compared to non-gradient optimization methods. However, gradient-based methods are accompanied by several drawbacks. Solution from a gradient-based method is not always a global minimum but a local minimum (Sun, 1994). Besides, an inversely computed field is apt to be over smoothed. In other words, local heterogeneity is hard to preserve although overall heterogeneity of the field are captured from the constrained number of observation data.

To overcome the problems above, a stochastic approach was employed in an optimization process. In addition, it is necessary to preserve spatial information of a field. Instead of adding the mean and standard deviation error terms to an objective function, the preservation of spatial information is accomplished by incorporating geostatistical methods into the optimization process. An inversed permeability field preserves the geostatistical properties such as mean, standard deviation, and covariance through the incorporation of geostatistical methods.

The stochastic optimization is composed of three modules, which are initial estimation by Kriging, primary gradient-based optimization by conjugate gradient method, and stochastic calibration. The procedure of the stochastic optimization in this study is summarized in Fig. 1, and description of the scheme is provided below in detail.

2.1. Initial estimate of permeability field

As most optimization methods are very sensitive to initial guess, it is effective to generate a field reflecting information of sample data. In the pilot point method and SSC, the inverse processes start with one realization of a conditionally simulated permeability field. It means that one probable field conditioned to sample data is chosen for an initial guess to be calibrated afterwards, and the methods require multiple runs on multiple conditionally simulated fields (RamaRao et al., 1995; Gomez-Hernandez et al., 1997). Consequently, the calibrated fields are also equi-probable selections of inversed fields and each calibrated field is dependent on each initial field. In addition, the inverse processes are computationally intensive due to multiple runs.

On the other hand, the stochastic optimization proposed in this study uses Kriging to generate an initial permeability distribution instead of conditional simulation such as SGS. Conditionally simulated fields can be considered to be fields with probabilistic randomness added to a Kriged field. Therefore, the Kriged field can be an unbiased average of conditionally simulated fields. An initial permeability distribution is obtained by ordinary Kriging, given a sample of permeability data. The characteristics of minimum error variance and unbiasedness allows Kriging to provide a good initial guess for a field incorporating information of sample permeabilities. The major trend of permeability distribution is captured through the initial guess provided through Kriging that minimizes the influence of initial guess on an inverse process as contrast to the SSC and the pilot point method.

2.2. Primary gradient-based optimization

The primary gradient-based optimization plays a significant role in efficiently reducing misfits between observation data and computed values, which continues to operate until the inverse process approaches a local minimum. The gradient-based optimization method can be expressed as,

$$k_{n+1} = k_n + \lambda_n d_n \tag{1}$$

where d_n is the displacement direction, and λ_n is the step size along that direction (Fletcher, 1993). From various gradient-based optimization schemes, the conjugate gradient method was employed. The Newton type methods such as Gauss Newton and Levenberg–Marquardt method, require construction of a Hessian matrix. In addition, the Newton type methods require solving a linear system involving the Hessian matrix in each iteration step. Therefore, these methods require huge storage requirements and computational time. On the other hand, the conjugate gradient method computes the displacement direction faster without calculating the Hessian matrix. It

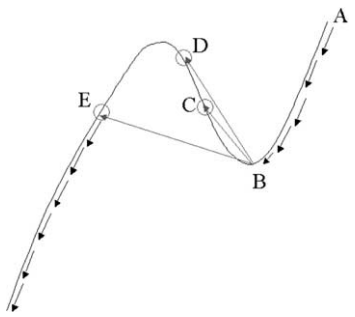

Fig. 2. Conceptual diagram of the stochastic calibration at a local minimum.

searches for the minimum by following mutually conjugate search directions (Yeh, 1986). It is expressed mathematically as

$$d_1 = -g_0, \qquad d_{n+1} = -g_n + \frac{g_n^T g_n}{g_{n-1}^T g_{n-1}} d_n \tag{2}$$

where g_n is the gradient vector at nth iteration step.

2.3. Stochastic calibration

If the gradient-based optimization process is trapped at a local minimum and the inverse process cannot proceed further, a stochastic simulation is applied. From the field caught in the local minimum, a number of releasing points are randomly selected. While the other points being conditioned, values are generated at the releasing points using SGS, honoring spatial characteristics of the existing field. This approach provides several equi-probable permeability fields conditioned to the permeability distribution that have been obtained by the inverse process up to that point. After that, one field that can reduce the objective function is selected from the equi-probable fields and the primary gradient-based optimization resumes its computation and proceeds to the next iteration step. Fig. 2 is a schematic diagram of stochastic calibration. The curve represents an objective function. The objective function is reduced by the gradient-based optimization from field A to field B. With field B, the objective function is unable to be reduced further by the gradient-based optimization, meaning the process is trapped at a local minimum. At this, field B is modified by the stochastic calibration and a realization C is generated as a result. Realization C is identical with field B except at the releasing points, where values are randomly generated by SGS. If the inverse process is unable to find the reduction of the objective function with realization C as well, another realization D is generated in the same way, being conditioned to field B. Stochastic calibration is repeated as above until the objective function can be reduced below that of field B with the generated field. With the realization E, the inverse process is able to find a direction along which the objective function is reduced below that of field B. Consequently, the inverse process escapes from the local minimum and gradient-based optimization is reactivated with field E.

During the inverse process, the inversed field is repeatedly calibrated and spatial characteristics are automatically incorporated by the stochastic calibration. Consequently, the stochastic optimization causes an inversed field to be calibrated by multiple realizations of conditional simulation internally and ultimately provides the most optimized field. When computed error becomes less than the error tolerance specified, the whole procedure is ended.

3. Adjoint state method for steady state flow with constant pressure boundary condition

The adjoint state method was used to compute displacement direction of parameters. By applying the adjoint state method, the derivative of the objective function with respect to a model parameter can be computed only through two flow simulations. If other methods such as the influence coefficient method and the sensitivity equation method are used, *number of parameters* + 1 simulations are required to calculate the gradient of the objective function (Yeh, 1986). Therefore, the accuracy of sensitivity calculation and computational speed can be considerably enhanced by the adjoint state method.

Adjoint state formulation is derived for the system, which has constant pressure injection and production wells under steady the state flow condition. The flow equation can be expressed as Eq. (3) and boundary condition as Eq. (4)

$$\nabla\cdot(T\nabla p) = 0 \tag{3}$$

$$p|_{\Gamma_0} = p_{\text{inj}}, \qquad p|_{\Gamma_1} = p_{\text{prd}}, \qquad (T\nabla p)\cdot n|_{\Gamma} = 0 \tag{4}$$

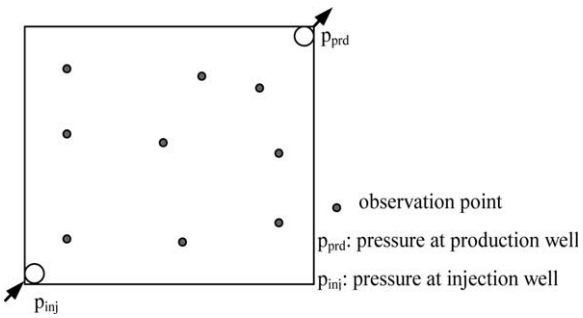

Fig. 3. Schematic diagram of flow system.

where T is kA/μ, p is the pressure, p_{inj} and p_{prd} are the pressure at injection and production well, respectively, Γ_0 is the injection point, Γ_1 is the production point, and Γ is the boundary.

From the above flow equation, an adjoint equation may be derived similarly as was done in several related works (Sykes, 1985; Sun and Yeh, 1990; Sun, 1994).

$$\nabla\cdot(T\nabla\psi) + \frac{\partial f}{\partial p} = 0 \tag{5}$$

$$\psi|_{\Gamma_0} = 0, \qquad \psi|_{\Gamma_1} = 0, \qquad (T\nabla\psi)\cdot n|_{\Gamma} = 0 \tag{6}$$

where ψ is the adjoint state parameter and f is the performance function.

Consequently, the error gradient can be calculated from Eq. (7)

$$\frac{\partial E}{\partial T} = \int_R \left(\frac{\partial f}{\partial T} - \nabla\psi\cdot\nabla p\right)\mathrm{d}R \tag{7}$$

where R is the spatial domain.

4. Streamline simulation

The main idea of streamline simulation is to decouple a multi-dimensional problem of fluid motion into multiple one-dimensional problems solved along streamlines. Fluids move along the natural streamline grid rather than between discrete gridblocks as in the conventional methods.

As with other conventional transport models, flow calculation is preceded in streamline simulation. The flow domain is then decomposed into a number of streamlines, and solute transport in each streamline is interpreted as a one-dimensional problem. Solving the one-dimensional transport problems analytically, we get the solutions along streamlines. Then, the solutions are remapped onto the original flow domain and the final concentration distribution is acquired as a function of location and time. This approach makes the streamline simulation eliminate the numerical dispersion error occurring in conventional finite difference methods and enhance calculation efficiency (Jang et al., 2002).

4.1. Coordinate transform along streamlines

The conventional Cartesian coordinate is converted into the coordinate system along streamlines through the concept of TOF (Crane and Blunt, 1999). Mathematically, TOF is defined as

$$\tau(s) = \int_0^s \frac{d\zeta}{v(\zeta)} \tag{8}$$

where ζ is the coordinate along a streamline.

4.2. Remapping to the Cartesian coordinate

An average gridblock concentration is calculated as the weighted average concentration in multiple streamlines that pass through it (Crane and Blunt, 1999; Thiele et al., 1996). The weighting in this calculation is determined according to the volume flux of each streamline

$$C_b = \frac{\sum_i q_i \Delta\tau_i C_i(\tau)}{\sum_i q_i \Delta\tau_i} \tag{9}$$

where C_b is the concentration in the gridblock, $\Delta\tau_i$ is the residence time in the gridblock along ith streamline, and q_i is the volume flux of ith streamline.

5. Model description

A synthetic permeability field was generated as a reference field using SGS. For the reference field, flow and transport simulations were conducted and information at observation points was monitored. Fig. 3 illustrates the schematic diagram of the flow system. Fluid is injected through the lowest left corner and produced at the upper right corner of the rectangular

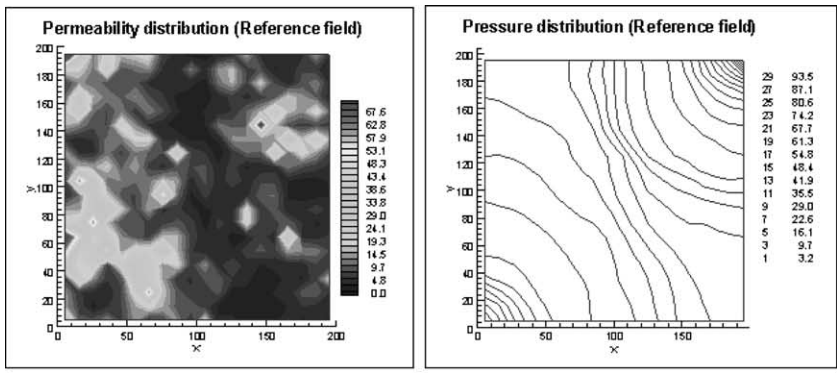

(a) Reference field

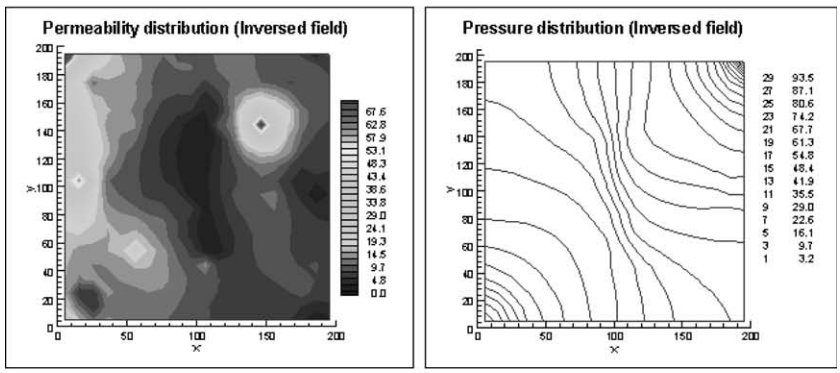

(b) By sole gradient-based method

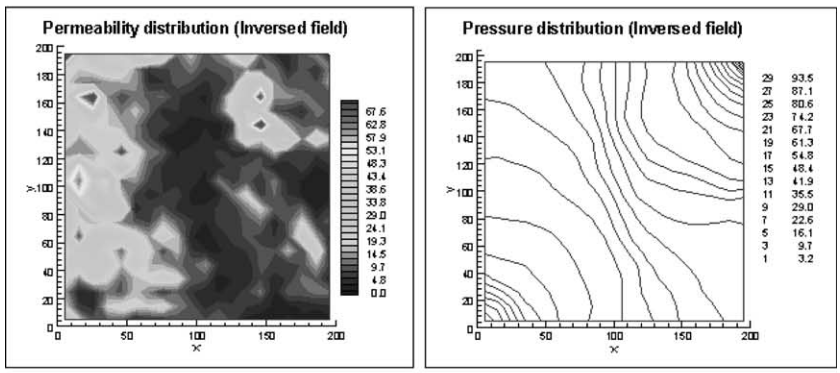

(c) By the stochastic optimization

Fig. 4. Permeability and pressure distributions for case 1. (a) The reference field, (b) results from a gradient-based optimization only, (c) results from the stochastic optimization.

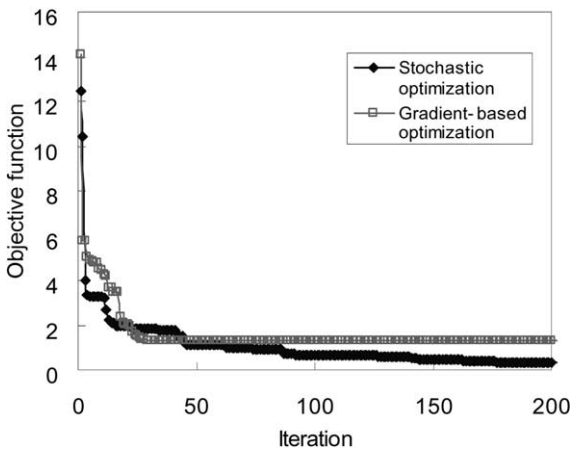

Fig. 5. Convergences of the objective function by the stochastic optimization and the gradient-based optimization.

grid system. No flow boundary conditions were applied to all the boundaries of the system.

5.1. Assumptions

The following simplifications were used to focus on the availability of the stochastic optimization. Permeability distributions were generated following a log-normal distribution and a exponential model was employed for the variogram. Porosity was assumed to be constant over the whole domain. Steady state flow condition was assumed and all the measurement data at the observation points were assumed to be free of errors.

5.2. Objective function

At the observation points, permeability and pressure data were obtained. Production rate was provided at the production well, which was also included in the sample point set. Accordingly, an objective function is expressed as follows

$$E = w_p \sum_{l=1}^{L} (p_l - p_l^{\text{obs}})^2 + w_k \sum_{l=1}^{L} (k_l - k_l^{\text{obs}})^2 + w_Q (Q - Q^{\text{obs}})^2 \quad (10)$$

where w is the weighting, l is the index of an observation point, L is the number of the observation points, p is the pressure, k is the permeability, and Q is the production rate. The objective function incorporates different types of information. p and Q are acquired from flow simulation and permeability samples provide spatial information of a field.

6. Results

Three synthetic permeability fields were generated, which have 20×20 gridblocks. Twenty-two observation points were set to report permeability and pressure measurements. The stochastic optimization was applied on the three fields and the following results were obtained over 500 iterations. To demonstrate applicability of the stochastic optimization, its results are compared with results by a sole gradient-based optimization.

6.1. Permeability and pressure distributions

Permeability and pressure distributions for case 1 are presented in Fig. 4. Fig. 4(a) is permeability and pressure distributions of the reference field, and Fig. 4(b) is solely a result of the gradient-based optimization. The inversed permeability field in Fig. 4(b) shows the overall trend of the permeability distribution of the reference field but it fails to show the spatial variability of the reference field. Although pressure distribution from flow simulation on the inversed field looks globally similar to that of the reference field, dissimilarity exists locally.

Fig. 4(c) shows the results from the stochastic optimization. It is observed that the major trend of the inversed permeability field honors that of the reference field. Moreover, variability at the local scale is well reflected in the inversed field, which is frequently over-smoothed by other inverse approaches based on the gradient-based methods as in Fig. 4(b). The pressure distribution of the inversed field reproduces that of the reference field very closely, and the matching with the pressure distribution of the reference field is enhanced compared to Fig. 4(b).

Fig. 5 presents comparison of the convergence between the stochastic optimization and the sole gradient-based method. Where the iteration number is over 30, the optimization process by the sole gradient-based method comes to be stuck in a local minimum

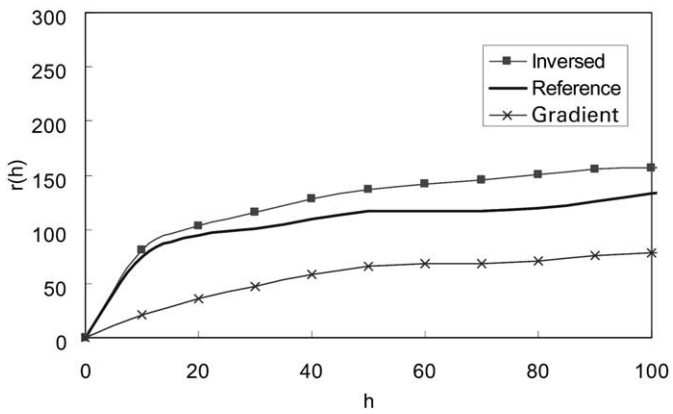

Fig. 6. Variograms of the reference field and the inversed fields.

and it is impossible to search for gradient directions along which the error is reduced. On the other hand, the error of the stochastic optimization continues to decrease even after the local minimum stage. This means that the stochastic optimization can overcome the local minimum problem and converge to a global minimum.

Variogram analyses of the permeability distribution were performed on the reference field and the inversed fields. The solid line in Fig. 6 represents a variogram of the reference field generated with a mathematical variogram model, and the rectangular points show a variogram of the inversed field by the stochastic optimization. It is observed that the variogram of the inversed field honors the variogram of the reference field. Both variogram curves of the reference and the inversed field begin to converge to sill value, where h is approximately 15, which is originally the correlation length value assumed for the mathematical variogram model. The inversed permeability field well reflects the spatial correlation of the reference field.

For the variogram of the inversed field by the sole gradient-based method, which is represented as cross points, it is observed that the standard deviation of the inversed field is less than that of the reference field. It again confirms that the inversed field only by a gradient-based method, is likely to be over-smoothed, and a mere gradient-based optimization is incomplete for reproducing spatial variability of an original field.

Table 1
Statistical summary for the reference field and the inversed field

Property	Reference field	Inversed field
Mean	10.78	13.12
Standard deviation	11.69	12.83
Coefficient of variation	1.084	0.978

Statistical parameters of the reference and inversed field are summarized in Table 1. Although regularization terms to match mean and standard deviation are not included in the objective function, mean and standard deviation of the inversed field are close to those of the reference field. In addition, the coefficient of variation in the inversed field is close to that in the reference field. This shows that the spatial variability of an unknown field can be reproduced by the stochastic optimization. These are due to the mechanism of the stochastic optimization that repeatedly generates spatially correlated values at releasing points, every time the process falls into a local minimum.

6.2. Prediction of future performance with the inversed field

To compare dynamic properties of the reference field and the inversed field, streamline simulation was performed on the both fields. We can efficiently investigate transport behavior of both fields by streamline simulation and evaluate how well the inversed field can predict future model performance.

Fig. 7 represents streamline trajectories and TOF distributions of the reference field (Fig. 7(a)) and the inversed fields (Fig. 7(b) and (c)). Since steady state flow condition was assumed, streamlines themselves represent paths along which particles move. It is

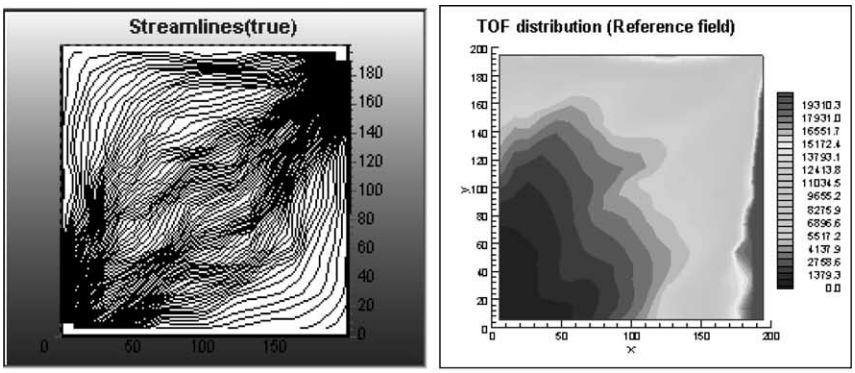

(a) Reference field

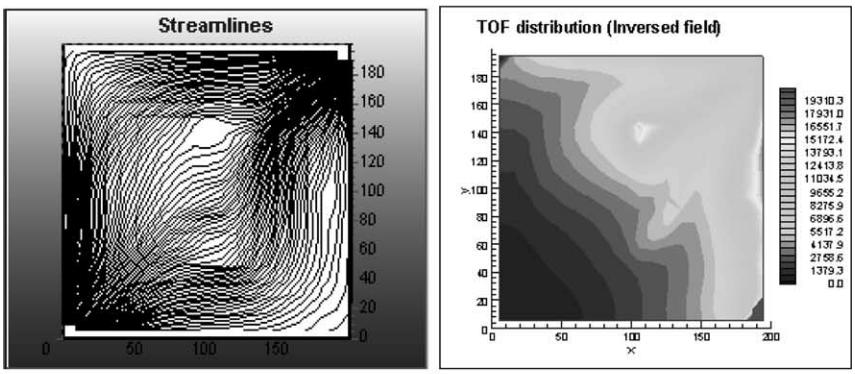

(b) By sole gradient-based method

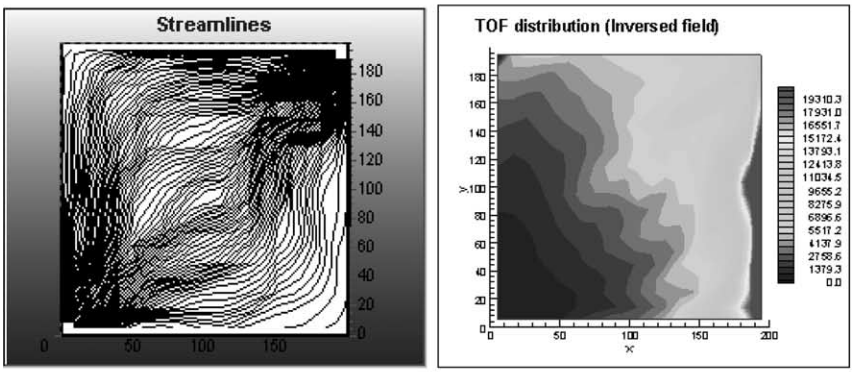

(c) By the stochastic optimization

Fig. 7. Streamline trajectories and TOF distributions. (a) Results of the reference field, (b) results by gradient-based method only, (c) results by the stochastic optimization.

observed that streamline trajectories of the stochastic optimization are more similar to those of the reference field than streamline trajectories by the sole gradient-based method. In Fig. 7(b), streamlines from the gradient-based method are distributed uniformly compared to the reference field. On the other hand, contrast in streamline population in Fig. 7(c) is more conspicuous than in Fig. 7(b). Streamlines are more closely spaced along fast paths as in the reference field (in Fig. 7(a)). The trajectories of streamlines from the

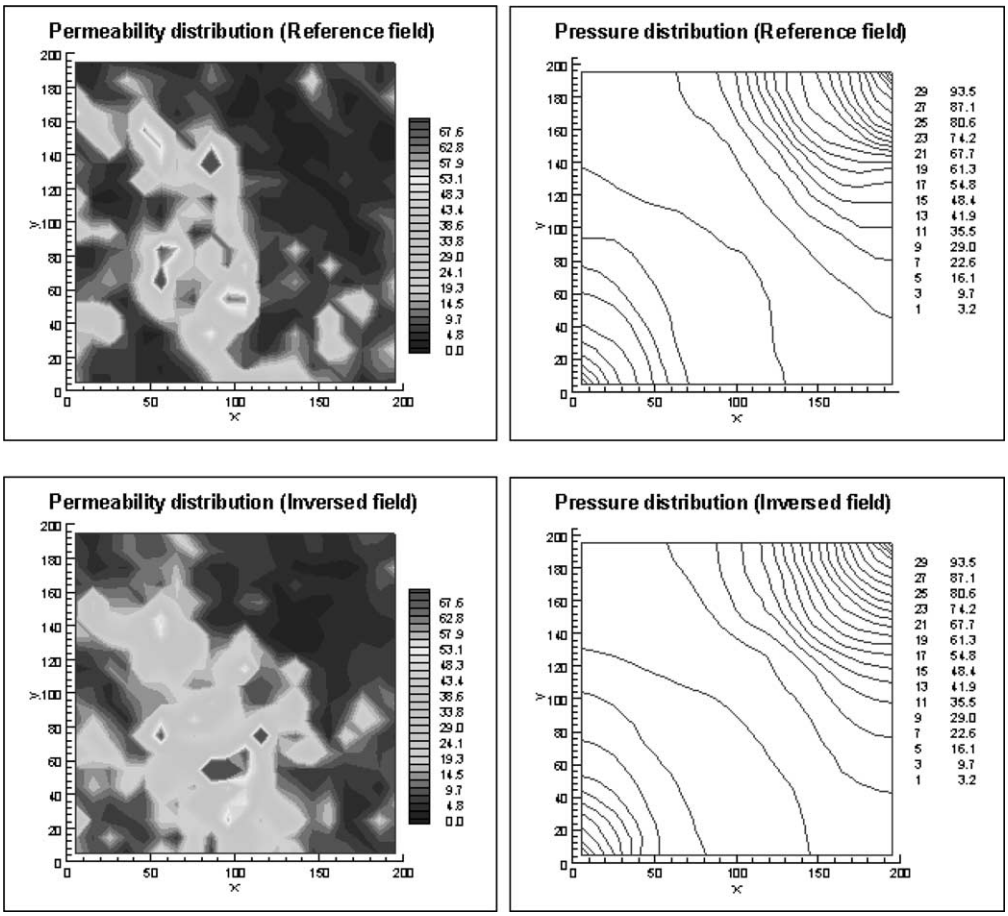

Fig. 8. Permeability distributions and pressure distributions for case 2. (a) The reference field, (b) the results from the stochastic optimization.

reference field and the inversed field are considerably analogous.

TOF denotes how long it takes for a particle to arrive at a specified position. In Fig. 7(b), TOF distribution by the gradient-based method is quite different from that of the reference field. While the contour lines of the reference field form pot-like shape in Fig. 7(a), those of the gradient-based method looks more like a right-angled triangle. This means that transport is predicted to propagate rapidly along the left and bottom boundaries, which does not coincide with the reference case in Fig. 7(a). However, TOF distribution predicted by the stochastic optimization reproduces the contour shapes of the reference field as shown in Fig. 7(c).

6.3. Applications to cases 2 and 3

The stochastic optimization was applied to another two synthetic fields, case 2 and case 3, in the same manner. The comparisons of permeability and pressure fields are presented in Figs. 8 and 9. In these cases, the inversed fields also reproduce unknown permeability and pressure field analogously as expected.

7. Conclusions

Simulation results indicate that unknown parameters in a field can be efficiently identified from a constrained number of permeability and pressure

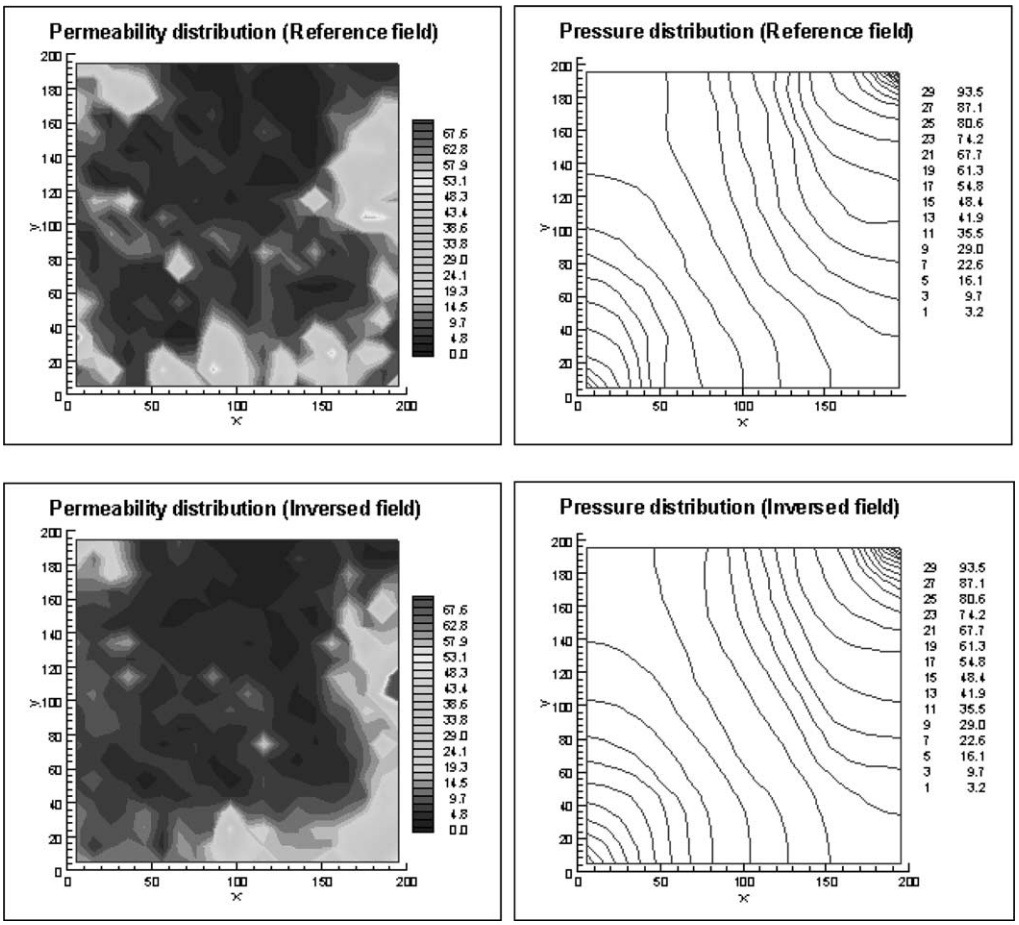

Fig. 9. Permeability distributions and pressure distributions for case 3. (a) The reference field, (b) the results from the stochastic optimization.

measurement data by the stochastic optimization. Being trapped at a local minimum, the stochastic optimization generates a number of equi-probable permeability distributions conditioned to the best parameter values available by that iteration stage. Through this approach, spatial characteristics of a field are automatically incorporated without adding regularization terms to an objective function. An inversed field preserves statistical properties such as mean and standard deviation of the original field, and reproduces spatial variability. In addition, pressure distribution and TOF distribution of the inversed field match those from the reference field. It enables the stochastic optimization to construct a reliable flow and transport model to predict future performance.

The stochastic optimization is fast in computation by using a gradient-based method as a primary optimization scheme and an adjoint state method in computation of sensitivity. It also guarantees global minimization by employing a geostatistical stochastic approach.

Acknowledgment

This research was conducted through the Research Institute of Engineering Science at Seoul National University, Korea and supported by KOSEF research project No. R01-2000-00058.

References

Batycky, R.P., Blunt, M.J., Thiele, M.R., 1997. A 3D field scale streamline-based simulator. SPE Reservoir Engng 12, 246–254.

Crane, M.J., Blunt, M.J., 1999. Streamline-based simulation of solute transport. Water Resour. Res. 35 (10), 3061–3077.

Datta-Gupta, A., Yoon, S., Barman, I., Vasco, D.W., 1998. Steamline-based production data integration into high resolution reservoir models. J. Pet. Technol., 72–75.

Deutsch, C.V., 1997. Geostatistical Software Library and User's Guide, Oxford University Press, New York.

Dogru, A.H., Seinfeld, J.H., 1981. Comparison of sensitivity coefficient calculation methods in automatic history matching. SPE J. 21, 551–557.

Fletcher, R., 1993. Practical Methods of Optimization, Wiley, New York.

Gomez-Hernandez, J.J., Sahuquillo, A., Capilla, J.E., 1997. Stochastic simulation of transmissivity fields conditional to both transmissivity and piezometric data-I. Theor. J. Hydrol. 203, 162–174.

Jang, M., Lee, J., Choe, J., Kang, J.M., 2002. Modeling of solute transport in a single fracture using streamline simulation and experimental validation. J. Hydrol. 261 (1-4), 74–85.

King, M.J., Datta-Gupta, A., 1998. Streamline simulation: a current perspective. In Situ 22 (1), 91–117.

McLaughlin, D., Townly, L., 1996. A reassessment of the groundwater inverse problem. Water Resour. Res. 32 (5), 1131–1161.

RamaRao, B.S., LaVenue, A.M., de Marsily, G., Marietta, M.G., 1995. Pilot point methodology for automated calibration of an ensemble of conditionally simulated transmissivity fields, 1. Theory and computational experiments. Water Resour. Res. 31 (3), 475–493.

Sun, N., 1994. Inverse Problems in Groundwater Modeling, Kluwer Academic Publications, Boston.

Sun, N., Yeh, W.W., 1990. Coupled inverse problems in groundwater modeling, 1. Sensitivity analysis and parameter identification. Water Resour. Res. 26 (10), 2507–2525.

Sykes, J.F., 1985. Sensitivity analysis for steady state groundwater flow using adjoint operators. Water Resour. Res. 21 (3), 359–371.

Thiele, M.R., Batycky, R.P., Blunt, M.J., Orr, F.M. Jr, 1996. Simulating flow in heterogeneous media using streamtubes and streamlines. SPE Reservoir Engng 10, 5–12.

Vasco, D.W., Yoon, S., Datta-Gupta, A., 1999. Integrating dynamic data into high-resolution reservoir models using streamline-based analytic sensitivity coefficients. SPE J. 4 (4), 389–399.

Wen, X.H., Clayton, D.V., Cullick, A.S., 1998. High resolution reservoir models integrating multiple-well production data. SPE J., 344–355.

Wen, X.H., Gomez-Hernandez, J.J., Capilla, J.E., Sahuquillo, A., 1996. Significance of conditioning to piezometric head data for predictions of mass transport in groundwater modeling. Math. Geol. 28 (7), 951–968.

Wu, Z., Reynolds, A.C., Oliver, D.S., 1999. Conditioning geostatistical models to two-phase production data. SPE J. 4 (2), 142–155.

Yeh, W.W.-G., 1986. Review of parameter identification procedures in groundwater hydrology: the inverse problem. Water Resour. Res. 22 (2), 95–108.

Zimmerman, D.A., de Marsily, G., Gotway, C.A., Marietta, M.G., Axness, C.L., Beauheim, R.L., Bars, R.L., Carrera, J., Dagan, G., Davies, P.B., Gallegos, D.P., Galli, A., Gomez-Hernandez, J., Grindrod, P., Gutjahr, A.L., Kitanidis, P.K., Lavenue, A.M., McLaughlin, D., Neuman, S.P., RamaRao, B.S., Ravenne, C., Rubin, Y., 1998. A comparison of seven geostatistically based inverse approaches to estimate transmissivities for modeling advective transport by groundwater flow. Water Resour. Res. 34 (6), 1373–1413.